This article has been accepted for inclusion in a future issue of this journal. Content is final as presented, with the exception of pagination.

Optomechanical Actuation of Diamagnetically Levitated Pyrolytic Graphite

Miriam Ewall-Wice[1], Steven Yee[1], Kelly DeLawder[1], Steven R. Montgomery[2], Peter J. Joyce[3], Cody Brownell[3], and Hatem ElBidweihy[1]

[1]Electrical and Computer Engineering Department, United States Naval Academy, Annapolis, MD 21402 USA
[2]Physics Department, United States Naval Academy, Annapolis, MD 21402 USA
[3]Mechanical Engineering Department, United States Naval Academy, Annapolis, MD 21402 USA

The magnetic susceptibility of pyrolytic graphite (PyG) is temperature dependent. Under an external magnetic field, a levitated PyG sample with a localized temperature change experiences unequal diamagnetic forces. In this paper, we present a study of the macroscale optomechanical displacement of a levitated PyG sample by using a laser source to locally increase the temperature. Dynamic finite-element method simulations show that a localized increase in the sample temperature, simulating a laser source, decreases the diamagnetic force in that local area, leading to the displacement of the PyG sample in the plane of the permanent magnet array. Experimental setups built using different laser sources and samples confirm the range of applicability of the actuation phenomenon to different conditions. An additional setup without moving parts reduced the likelihood by which airflow could have caused the displacement, as we suspect happened in the previous studies.

Index Terms—**Diamagnetic levitation, optomechanical actuation, pyrolytic graphite (PyG).**

I. Introduction

OPTOMECHANICAL actuators have gained renewed interest in the past decade. Nanoscale devices that exhibit mechanical displacement or a change in shape when illuminated by light have been designed [1], [2]. A comprehensive review of the optomechanical effect can be found in [3]. Optomechanical actuation using diamagnetic materials has not been deeply investigated in the literature.

The magnetic susceptibility of certain diamagnetic materials changes photothermally because of the increase in the number of thermally excited electrons. Several studies have presented various forms of actuation by exploiting the diamagnetic properties of pyrolytic graphite (PyG) [4]–[6]. A micromachined graphite rotor was levitated over an array of concentric permanent magnets setup consisting of an outer cylindrical magnet with a hollow center and an inner cylindrical magnet of the opposite polarization [7]. The rotation of the graphite rotor resulted from air flowing from a needle-thin gas nozzle to spin the rotor. A viscometer composed of a free-spinning graphite disk over top the magnet array was presented [8].

A limited number of studies have used the temperature-dependent diamagnetic properties of PyG to achieve mechanical displacement. The use of a laser beam as an ON/OFF switch for a possible maglev system using PyG was proposed [9]. Rather than directly irradiating the PyG sample, a temperature-dependent ferrite was laser heated causing the PyG sample to move toward it [10]. The weakened magnetic field around the heated ferrite caused the graphite sample to move toward the ferrite, but not through direct irradiation. Microscale vertical displacement of PyG irradiated by laser powers between 20 mW and 1 W was proposed as a method for sensing the laser power magnitude [11].

The first reported effort to harness the photothermal change in the diamagnetism of PyG to achieve macroscale displacement used a 405 nm, 300 mW laser to control the horizontal displacement of a 150 μm-thick 3 mm-diameter PyG disk, reaching a maximum velocity of 45 mm/s [12].

In this paper, we present a detailed study of the macroscale optomechanical response of PyG levitated on a 12×6 array of 6.35 mm $\times$ 6.35 mm cylindrical NdFeB permanent magnets of alternating polarity. The PyG samples, acquired from different sources, exhibit temperature-dependent magnetic susceptibility. Optical components are used to focus the laser beam on a specific location on the PyG sample to create a temperature gradient leading to unbalanced levitation and horizontal displacement.

Initially, the setup in [12] was replicated and horizontal displacement was achieved but not because of the sought-after reason. We discovered that the airflow from the cooling fan attached to the heat sink housing was the primary reason for the displacement of the sample, concealing the effect of the laser irradiation on the local temperature. When our replication of the setup in [12] was modified only by blocking airflow from the fan attached to the laser, no displacement was observed with the laser powers and sample dimensions reported. Our subsequent experiments focused on eliminating the unintended airflow and to present the first detailed study of the optomechanical displacement of diamagnetically levitated PyG. We used various laser types, wavelengths, and powers, without fan attachments, to displace two different PyG samples levitating above permanent magnet arrays. Finite-element method simulations are presented in Section II-C to support the proposed concept of actuation described in Section II-A. Due to difficulties in mesh development for very

Manuscript received October 31, 2018; revised December 13, 2018; accepted December 28, 2018. Corresponding author: H. ElBidweihy (e-mail: elbidwei@usna.edu).

Digital Object Identifier 10.1109/TMAG.2019.2892332

This article has been accepted for inclusion in a future issue of this journal. Content is final as presented, with the exception of pagination.

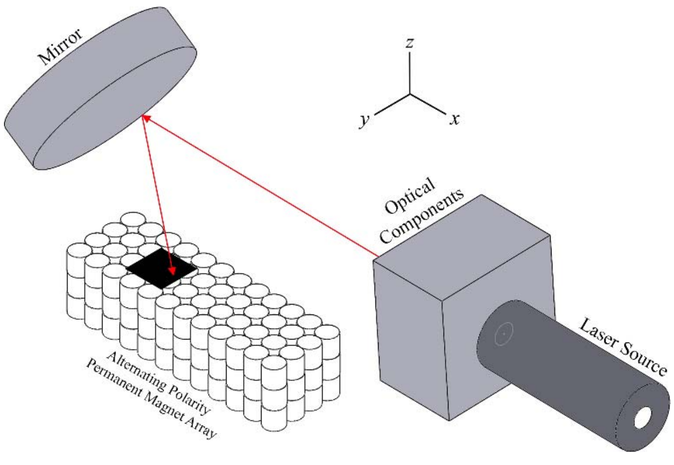

Fig. 1. Schematic of a typical experimental setup used in this paper to characterize the optomechanical response of a magnetically levitated sample of PyG.

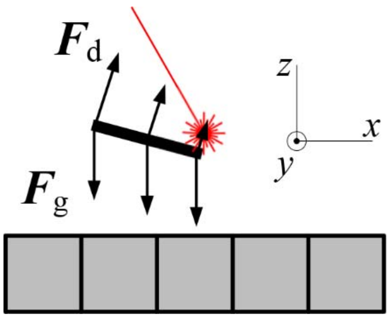

Fig. 2. Schematic showing PyG (black sample) levitating above a permanent magnet array (gray blocks). Laser irradiation localized to one end of the graphite results in an imbalance between the anisotropic diamagnetic force $\boldsymbol{F}_d$ and the gravitational force $\boldsymbol{F}_g$ due to the temperature dependence of the former. The imbalance of the volumetric forces results in a tilt in the graphite sample. The use of multiple arrows to depict each of the forces illustrates the non-uniform force distribution resulting from the localized laser heating.

thin PyG samples, the dimensions used in the simulations do not match the specifications for the experiments reported in Section III. However, the results of the simulations using scaled laser powers and thicknesses confirm the proposed general concept explaining the observed optomechanical effect.

II. Device Design

A. Concept

Diamagnetic materials develop negative magnetic moments opposing externally applied magnetic fields. PyG exhibits the greatest diamagnetism by weight at room temperature and has been used in levitation applications since 1966 [13]. In the presence of strong magnetic fields, PyG samples can easily attain stable levitation at room temperature with no power consumption.

The diamagnetic force $\boldsymbol{F}_d$ induced by an external magnetic field is given by

$$\boldsymbol{F}_d = \iiint \nabla(\boldsymbol{B} \cdot \boldsymbol{M}) dV \tag{1}$$

where $\boldsymbol{B}$ is the magnetic flux density through the volume V, and $\boldsymbol{M}$ is the magnetization given by

$$\boldsymbol{M} = \chi \boldsymbol{H} \tag{2}$$

where $\boldsymbol{H}$ is the magnetic field strength and χ is the volumetric susceptibility. For a vertically stable levitation, the magnetic force is equal to the gravitational force $\boldsymbol{F}_g$ leading to

$$mg = \frac{\chi V}{\mu_0} \nabla \boldsymbol{B}^2 \tag{3}$$

where g is the gravitational constant, and m and V are the mass and the volume of the diamagnetic sample, respectively.

A slight tilt can be induced in a PyG sample when its magnetic susceptibility is locally altered by a local change in sample temperature. Laser irradiation can be focused on a certain spot on the sample to induce the local temperature change, as shown in the schematic experimental setup in Fig. 1.

The local imbalance of gravitational and diamagnetic forces results in a moment that induces a tilted position at which the local gravitational and diamagnetic forces are balanced. Consider the schematic in Fig. 2. Prior to exposure to a heat source, the z-axis is perpendicular to the plane of the sheet and is the primary axis of magnetization. With a local variation in the susceptibility and a resulting tilt, the primary axis of magnetization remains normal to the plane of the PyG, which is no longer parallel with the z-axis. This shift in the magnetization axis results from the anisotropy of susceptibility of PyG, in addition to its temperature dependence. PyG is significantly more diamagnetic in the direction normal to the surface of a PyG sheet than parallel to the surface. Therefore, the resulting diamagnetic force on a PyG sheet with an induced tilt has x-, y-, and z-component. The x- and y-component of the diamagnetic force result in translational movement of the PyG. Laser heating is well suited to induce this translational movement because the applied heat is localized and can be precisely controlled while avoiding physical contact that would restrict any resulting motion.

B. Pyrolytic Graphite

Two commercial PyG materials with superior in-plane thermal transport properties have been used in the experiments presented in this paper. The first material is a 1 mm-thick rigid pyrolytic graphite disk (PGD) from Goodfellow Corporation. The second one is a 25 μm-thick flexible pyrolytic graphite sheet (PGS) from Panasonic. Their in-plane thermal conductivities and densities are 1.6 and 0.3 kW/(m $\cdot$ K) and 2.2 and 1.90 g/cm^3, respectively. PyG exhibits large diamagnetism with a relative permeability of 0.9996 and a magnetic susceptibility $\chi = -4\times10^{-4}$. The measured magnetic moment per unit mass of the two samples under an external magnetic field of 0.5 T applied perpendicular to the plane of the sample shows a decreasing negative susceptibility with increasing temperature as shown in Fig. 3.

C. Simulations

Finite-element simulations were carried out in COMSOL Multiphysics in order to improve understanding of the dynamic interplay of the thermal and magnetic physics underlying the

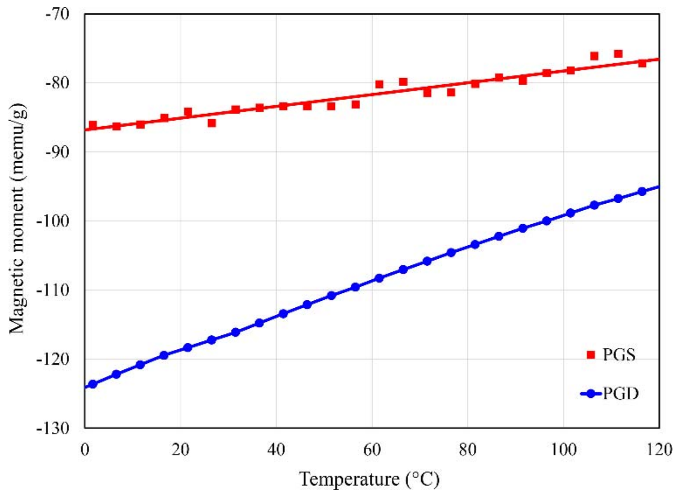

Fig. 3. Measured magnetic moment per unit mass versus temperature for two PyG samples under an external magnetic field of 0.5 T. The measurements were done using a vibrating sample magnetometer. The masses of the PGS and PGD samples measured were 0.0015 and 0.057 g, respectively.

actuation phenomena and confirm the conceptual explanation for displacement due to incident laser radiation. The simulations serve as a foundation for future design of optomechanical actuators based on photothermally varying diamagnetism. For simplicity in the development of a conceptual model, thin layers have been avoided, and input laser powers and permanent magnet strengths have been scaled upward accordingly.

The simulation geometry features a three-layer, 2×2 array of 20 mm $\times$ 20 mm $\times$ 3 mm NdFeB rectangular magnets arranged in an opposite neighboring poles configuration along the *xy*plane. A 1 mm-thick 15 mm $\times$ 15 mm PyG sample is centered above the array at an arbitrary height of 0.8 mm. The model geometry is completed by a spherical domain of air with a diameter of 200 mm and a spherical shell domain of infinite elements with a thickness of 10 mm. The last domain improves the computational efficiency of the simulation.

The magnetic phenomena are modeled using COMSOL ac/dc's magnetic fields no currents module. A magnetic remanence of 2 T is assumed for modeling purposes for each NdFeB magnet. The graphite sheet is modeled as a magnetized solid domain, where the magnetization $\boldsymbol{M}$ is computed as in (2). The susceptibility χ is defined as a temperature-dependent function with differing values in the direction normal to the face of the sheet ($\chi_{\perp}$) and parallel with the sheet ($\chi_{\parallel}$). This anisotropy in the susceptibility of PyG is based on [14], [15], and the temperature dependence of the susceptibility was experimentally verified. Susceptibility is modeled according to the following functions:

$$\chi_{\perp} \times 10^6 = -743 + T \tag{4}$$
$$\chi_{\parallel} \times 10^6 = -135 + 0.25T \tag{5}$$

where T is the temperature in Kelvin and χ is unitless (SI).

Due to the anisotropy of the susceptibility, the magnetization is computed within the material frame for the model and recomputed within that frame when motion is simulated. However, the magnetization of the sample is available in the global spatial frame of reference (x-, y-, and z-coordinate) following the computation in the material frame of reference. Therefore, in general, the diamagnetic force must account for x-, y-, and z-component since the material will not remain parallel to the magnet array throughout the simulation.

The diamagnetic force is derived from (1) and is implemented in COMSOL's *Solid Mechanics* module as a volumetric body force. Whereas the magnetization is initially calculated in the material frame, the diamagnetic force can be calculated in the global spatial frame with the forces in the spatial x-, y-, and z-direction as follows:

$$f_x = \iiint \frac{d}{dx}(B_x M_x + B_y M_y + B_z M_z) dV \tag{6}$$
$$f_y = \iiint \frac{d}{dy}(B_x M_x + B_y M_y + B_z M_z) dV \tag{7}$$
$$f_z = \iiint \frac{d}{dz}(B_x M_x + B_y M_y + B_z M_z) dV. \tag{8}$$

The computation of x- and y-directed forces is necessary to model the translational components of the diamagnetic force that come into effect after a tilt in the graphite is initiated by a localized decrease in the diamagnetic force opposing gravity. Gravity is also applied as a body force within the solid mechanics module and is calculated from the dimensions and the density of the graphite sample which is modeled as 1.9 g/cm^3.

Laser heating of the graphite is implemented using COMSOL's heat transfer in solids module. A deposited beam power with a Gaussian profile is arbitrarily modeled as sweeping across the surface of the graphite at a speed of 10 mm/s. For conceptual purposes, a beam power of 100 W is used. Thermal conductivity of graphite sheet is modeled as 1000 W/m·K in the x-and y-direction and 700 W/m·K through the thickness of the graphite. The heat capacity is modeled as a constant 1 J/g · K.

To enable simulated displacement of the graphite, a Moving Mesh module is implemented in COMSOL with a prescribed mesh displacement deriving from the displacement field calculated in the Solid Mechanics module. The entire simulation is coupled together by the temperature response to laser heating input, the temperature dependence of the magnetic susceptibility, and the displacement resulting from a magnetization-dependent force. Time-dependent simulation results successfully demonstrated both stable levitation and optomechanical actuation of the described simulation setup as a result of laser heating as shown in Fig. 4.

The simulation results exhibit some ringing of the vertical position of the graphite at the start of the simulation and a small net increase in its levitation height above the magnet array relative to the arbitrary levitation height initially set in the model. This increase in levitation height is due solely to an underestimation of the diamagnetic levitation force in the initial model setup and demonstrates the correct levitation modeling in the simulation. The translational effect is observed in simulations after the laser beam strikes the surface of the graphite and begins to translate. A small tilt is induced in the graphite that continues to increase as the laser beam translates

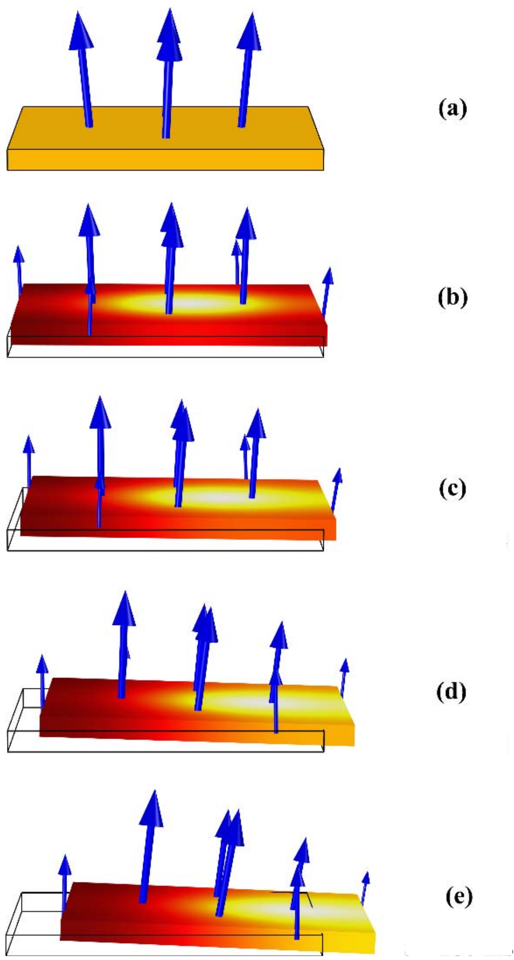

Fig. 4. Simulation results from the top to the bottom at (a) $t = 0$ s, (b) $t = 75$ ms, (c) $t = 150$ ms, (d) $t = 225$ ms, and (e) $t = 280$ ms showing graphite sheet actuation. Blue arrows are proportional representations of the calculated diamagnetic force at the simulation time. Surface coloring of the graphite sheet represents relative temperature on the graphite sheet surface, which reflects the movement of applied laser heating from the center to the right edge of the sample over time. Maximum temperature is 362 K, and the minimum is 326 K in (e). Local decreases in the diamagnetic force with increasing temperature and the shift in the magnetization axis are observable. The resulting rightward displacement of the sample (amplified by a factor of 3) is shown along with the starting position of the sample.

closer to the edge of the graphite. The resulting translational motion is of the same type as that observed in experiments.

III. Experiment

The first experiment was set up to replicate the study in [12]. A 250 μm-thick PGD sample moved smoothly using a 405 nm, 500 mW laser diode. The laser, commonly used by hobbyists for engraving applications, is housed within a large heat sink with a cooling fan attached. Several lab-grade lasers within the same power range but of different wavelengths (638, 976, and 1064 nm) were tested and were not successful in displacing the PGD sample. The 405 nm wavelength was immediately presumed to be a necessary factor for displacement, but the optical absorption of PyG was found to exhibit very small wavelength dependence for wavelengths above 400 nm (resonance occurs around 270 nm) [16]. Lasers with 458 and 488 nm wavelength and power levels up to 2 W were tested on the same sample and were also not successful in causing displacement. Further investigation revealed that the reason for the effortless displacement achieved in [12] is the airflow from the cooling fan attached to the heat sink housing.

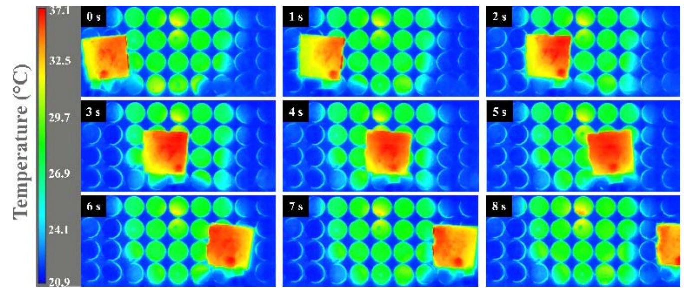

Fig. 5. 9 s sequence of infrared thermal images captured as a 975 nm, 330 mW laser is moving along the edge of a PGS sample from the left to the right. The sample's surface area is 12 mm × 12 mm, and the diameter of the cylindrical permanent magnets is 6.35 mm.

Realizing that the laser wavelength is not a determining factor for achieving displacement, the focus was shifted to developing or purchasing thinner samples and to use higher laser power levels. The 25 μm PGS samples were displaced using Fiber–Bragg–Grating stabilized laser diodes with wavelengths and powers of 976 nm–300 mW, 975 nm–330 mW, and 976 nm–500 mW. The PGD samples, sanded to 140 μm, were displaced using a tunable continuous wave (CW) argon ion laser with wavelengths and powers of 458 nm–2 W and 488 nm–2 W.

Two experimental setups similar to Fig. 1 were built to test the optomechanical response of PyG using various laser sources and samples to confirm the range of applicability of the actuation phenomenon to different conditions.

In the first setup, a 975 nm, 330 mW fiber-coupled laser mounted on a manual translational stage irradiated a PGS sample (7 mg, 12 mm × 12 mm × 25 μm). In the second setup, a 488 nm, 2 W tunable CW argon ion laser irradiated a PGD sample (30 mg, 13 mm × 13 mm × 140 μm) through a mirror mounted on a manual translational stage and aimed at the sample. The magnet array is comprised 12×6 6.35 mm × 6.35 mm cylindrical NdFeB permanent magnets of alternating polarities with a maximum magnetic field of 0.5 T at the surface.

At an incidence angle of 45° and 40° and a translational speed of 8.5 and 10.5 mm/s for the first and second setups, respectively, moving the laser along an edge of the sample displaced it in the same direction as the movement of the laser at an average speed of 7.7 and 18 mm/s, as shown in the thermal images in Figs. 5 and 6. The large difference between the translational speed of the laser and the sample displacement speed is due to the "jerk-like" displacement of the PGD sample.

The difference between the maximum and minimum sample temperature is 10 °C and 30 °C for the PGS and PGD samples, respectively, as shown in Figs. 5 and 6. This larger sample temperature gradient results in a larger magnetic susceptibility change which leads to a greater translational component of the diamagnetic force in the plane of the magnet array,

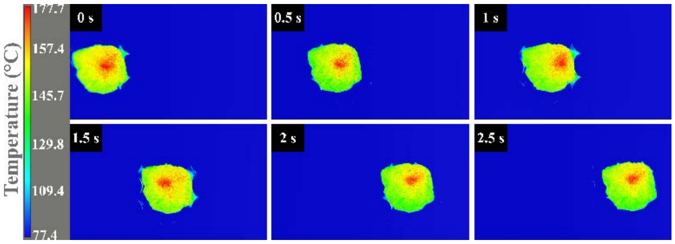

Fig. 6. 3 s sequence of infrared thermal images captured as a 488 nm, 2 W laser is moving along the edge of a PGD sample from the left to the right. The sample's surface area is 13 mm × 13 mm.

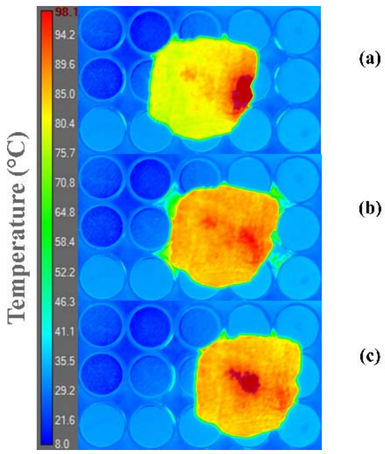

Fig. 7. 1 s sequence of infrared thermal images captured as a stationary 488 nm, 2 W laser is irradiating a PGD sample through a 1 Hz optical chopper. The sample's surface area is 13 mm × 13 mm, and the diameter of the cylindrical permanent magnets is 6.35 mm. Irradiating the edge of sample for 0.5 s displaced it by approximately 6.35 mm. (a) $t = 0$ s laser ON. (b) $t = 0.5$ s laser OFF. (c) $t = 1$ s laser ON.

compared to the PGS sample. A relatively low-power laser (330 mW) was sufficient to displace the thin PGS sample, but a higher power laser (2 W) was required to displace the thicker PGD sample.

In order to avoid having airflow be part of the experiment, as in previous studies, a simple experiment was set up with no moving parts. The laser and mirror were fixed and a 1 Hz optical chopper was used to irradiate the sample for an interval of 0.5 s. Upon the first instant of irradiation on the edge of the sample, a large sample temperature gradient is produced, which displaced the sample to the next favorable minimum magnetic field on the magnet array, as seen in Fig. 7(a). The superior thermal properties of PyG dissipated the heat through the entire sample, causing the sample to slow down [Fig. 7(b)] and finally stop when the irradiation spot is in the center of the sample [Fig. 7(c)].

Higher irradiation chopping frequencies lead to the sample oscillating in place and never moving to the next point of minimum magnetic field, suggesting the existence of a resonance-like process connecting the laser power and chopping frequency to the thermal properties of the sample.

It should be noted that several aspects of the experiment have to work together harmoniously to achieve effortless actuation. The tilt initiates the displacement but as the sample moves the problem becomes more complex. The magnetic field the sample is experiencing is changing and the geometry is not tightly controlled. Future work will include using computer-controlled translational fixtures to achieve repeatable results and to further study the complexity of the resulting movement.

IV. Conclusion

This paper presented a preliminary study investigating the displacement of PyG levitated above a permanent magnet array and irradiated by a laser source. An analytical explanation was presented for this actuation phenomenon based on the temperature dependence of magnetic susceptibility, the anisotropy of the diamagnetic effect, and a subsequent redirection of the diamagnetic force in PyG. The temperature dependence of the diamagnetism of PyG was experimentally verified. Successful levitation and actuation were observed in two experimental setups using different samples, laser power levels, and wavelengths to confirm the range of applicability of the actuation phenomenon to different conditions. Unlike [12], our experiments were designed to eliminate specimen displacement due to unintended airflow and demonstrated that while the optomechanical effect claimed in [12] was partly verified, the required laser power for actuation was significantly higher than that reported for PyG of similar dimensions. Unlike previous simulations concerning diamagnetic levitation [5], [9], [12], [14], our simulations are time dependent and account for localized changes in diamagnetism. Dynamic simulations are required to assess the transient thermal effects of laser irradiation as well as the movement of both the laser and the PyG sample.

The conceptual explanation and experimental findings were supported by finite-element method simulations. Continued simulation work aims to expand beyond conceptual confirmation by tailoring modeling parameters to specific experimental setups and predicting the combinations of materials, dimensions, laser powers, and laser movements that will result in a particular displacement.

Acknowledgment

This work was supported in part by the Naval Academy Bowman Scholar Program, in part by the Department of the Navy Science and Engineering Apprenticeship Program, and in part by the Office of Naval Research.

References

[1] Z. Liu *et al.*, "Nanoscale optomechanical actuators for controlling mechanotransduction in living cells," *Nature Methods*, vol. 13, no. 2, pp. 143–146, 2015.

[2] P. R. Leeladhar and J. P. Singh, "Sunlight-driven eco-friendly smart curtain based on infrared responsive graphene oxide-polymer photoactuators," *Sci. Rep.*, vol. 8, no. 1, 2018, Art. no. 3687.

[3] T. Ube and T. Ikeda, "A historical overview of photomechanical effects in materials, composites, and systems," in *Photomechanical Materials, Composites, and Systems*, T. J. White, Ed. Hoboken, NJ, USA: Wiley, 2017, doi: 10.1002/9781119123279.ch1.

[4] G. Küstler, "Simultaneous inline triple levitation in diamagnetic levitation system with permanent magnets," *Electron. Lett.*, vol. 51, no. 15, pp. 1172–1174, 2015.

[5] C. Niu, F. Lin, Z. M. Wang, J. Bao, and J. Hu, "Graphene levitation and orientation control using a magnetic field," *J. Appl. Phys.*, vol. 123, no. 4, p. 044302, 2018.

[6] X. Han and J. Li, "Maglev rotating disk laser," *Chin. Opt. Lett.*, vol. 13, no. 12, p. 121403, 2015.

[7] Y. Su, Z. Xiao, Z. Ye, and K. Takahata, "Micromachined graphite rotor based on diamagnetic levitation," *IEEE Electron Device Lett.*, vol. 36, no. 4, pp. 393–395, Apr. 2015.

[8] Y. Shimokawa, Y. Matsuura, T. Hirano, and K. Sakai, "Gas viscosity measurement with diamagnetic-levitation viscometer based on electromagnetically spinning system," *Rev. Sci. Instrum.*, vol. 87, no. 12, p. 125105, Dec. 2016.

[9] S. Kang, J. Kim, J.-B. Pyo, J. H. Cho, and T.-S. Kim, "Design of magnetic force field for trajectory control of levitated diamagnetic graphite," *Int. J. Precis. Eng. Manuf.-Green Technol.*, vol. 5, no. 2, pp. 341–347, Apr. 2018.

[10] Y. Mizutani, A. Tsutsumi, T. Iwata, and Y. Otani, "Optically driven method for magnetically levitating diamagnetic material using photothermal effect," *J. Appl. Phys.*, vol. 111, no. 2, p. 023909, Jan. 2012.

[11] P. Pinot and Z. Silvestri, "New laser power sensor using diamagnetic levitation," *Rev. Sci. Instrum.*, vol. 88, no. 8, p. 085003, 2017.

[12] M. Kobayashi and J. Abe, "Optical motion control of Maglev graphite," *J. Amer. Chem. Soc.*, vol. 134, no. 51, pp. 20593–20596, 2012.

[13] R. D. Waldron, "Diamagnetic levitation using pyrolytic graphite," *Rev. Sci. Instrum.*, vol. 37, no. 1, pp. 29–35, 1966.

[14] C. S. Siyambalapitiya, "Model and validation of static and dynamic behavior of passive diamagnetic levitation for energy harvesting," Ph.D. dissertation, Dept. Elect. Eng., College Eng., Univ. South Florida, Tampa, FL, USA, 2012.

[15] M. D. Simon, L. O. Heflinger, and A. K. Geim, "Diamagnetically stabilized magnet levitation," *Amer. J. Phys.*, vol. 69, no. 6, pp. 702–713, 2001.

[16] G. I. Dovbeshko *et al.*, "Optical properties of pyrolytic carbon films versus graphite and graphene," *Nanosc. Res. Lett.*, vol. 10, no. 1, p. 234, 2015.